ACS Energy LETTERS

http://pubs.acs.org/journal/aelccp

Rapid Recombination by Cadmium Vacancies in CdTe

Seán R. Kavanagh, Aron Walsh,* and David O. Scanlon*

Cite This: *ACS Energy Lett.* 2021, 6, 1392−1398

Read Online

ACCESS | Metrics & More | Article Recommendations | Supporting Information

ABSTRACT: **CdTe is currently the largest thin-film photovoltaic technology. Non-radiative electron−hole recombination reduces the solar conversion efficiency from an ideal value of 32% to a current champion performance of 22%. The cadmium vacancy (V_{Cd}) is a prominent acceptor species in *p*-type CdTe; however, debate continues regarding its structural and electronic behavior. Using *ab initio* defect techniques, we calculate a negative-U double-acceptor level for V_{Cd}, while reproducing the V_{Cd}^{1-} hole−polaron, reconciling theoretical predictions with experimental observations. We find the cadmium vacancy facilitates rapid charge-carrier recombination, reducing maximum power-conversion efficiency by over 5% for untreated CdTe—a consequence of tellurium dimerization, metastable structural arrangements, and anharmonic potential energy surfaces for carrier capture.**

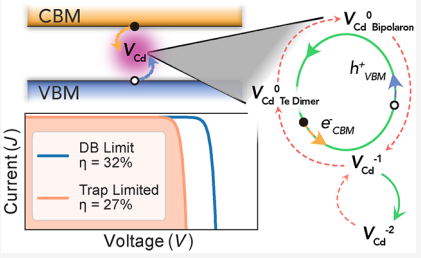

Cadmium telluride (CdTe) is a well-studied thin-film photovoltaic (PV) absorber, being one of few solar technologies to achieve commercial viability.[1] Its ideal 1.5 eV electronic band gap and high absorption coefficient have allowed it to reach record light-to-electricity conversion efficiencies of 22.1%.[2−4] Given that device architectures and large-scale manufacturing procedures have been highly optimized for this technology—a result of several decades of intensive research[2,5]—further reductions in cost will be heavily dependent on improvements in photoconversion efficiency.[1,2,6] Indeed, under the idealized detailed balance model, CdTe has an upper limit of 32% single-junction PV efficiency (based on its electronic bandgap),[7] indicating that there is still room for improvement.[6,8−11]

Despite over 70 years of experimental and theoretical research,[2,12−19] the defect chemistry of CdTe is still not well understood. The unambiguous identification of the atomistic origins of many experimentally observed spectroscopic signatures remains elusive. Only through clear understanding of defect behavior can strategies be devised to avoid and/or mitigate their deleterious effects on device performance.[20−23]

At present, market-leading CdTe solar cells employ a Te-rich *p*-type CdTe absorber layer, favoring the formation of Cd vacancies. Indeed, *undoped* CdTe grown from the melt is typically found to exhibit native *p*-type behavior,[14] which has often been attributed to the presence of vacancies in the Cd sub-lattice (and/or Te-on-Cd antisites).[18] However, the exact origin of this low intrinsic *p*-type conductivity is still not well understood, with difficulties in definitive measurements[14−16,24] and discrepancies between models and observations.[2,25−28] While there is consensus that the cadmium vacancy (V_{Cd}) is an important acceptor species in CdTe, strong debate has endured regarding its structural and electronic behavior.[2,14,18,26−32]

The ability of modern theoretical approaches to accurately describe defect behavior is well established.[20,33,35] The use of a sufficiently accurate Hamiltonian is essential for reliable predictions. For CdTe, using a screened hybrid Density Functional Theory (DFT) functional with spin−orbit coupling (HSE+SOC), we find that the room-temperature experimental bandgap of 1.5 eV is reproduced at a Hartree−Fock exchange fraction α_{exx} = 34.5%, a value which also reproduces the experimental lattice constant to within 1% (see Supporting Information). For consistency, this model was employed in all structural optimizations and electronic calculations.

Cadmium Vacancy: Equilibrium Structures. The first step in any theoretical investigation of solid-state defects is the determination of their equilibrium structures. CdTe crystallizes in the zinc-blende structure (space group $F\bar{4}3m$), thus exhibiting tetrahedral (T_d) symmetry at both the Cd and Te sites. The relaxed geometric configurations upon creation of a cadmium vacancy in the neutral (V_{Cd}^{0}), single-negative (V_{Cd}^{1-}), and double-negative (V_{Cd}^{2-}) charge states are shown in Figure 1. Only the double-negative defect retains the original tetrahedral point-group site symmetry, with a contraction of the

Received: February 19, 2021
Accepted: March 12, 2021
Published: March 19, 2021

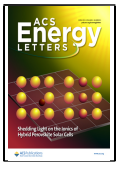

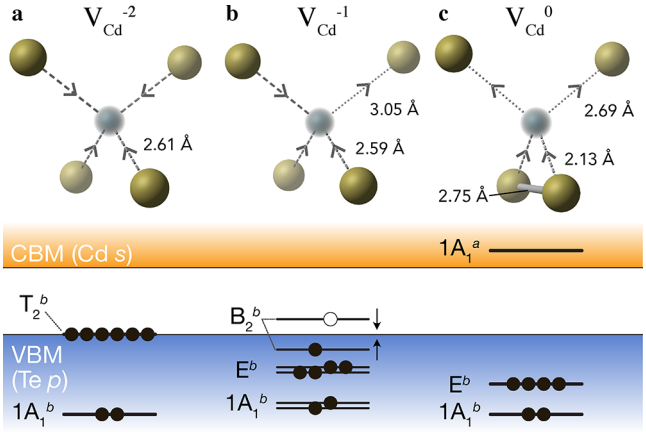

Figure 1. (Top) Ground-state structures of the cadmium vacancy in the double-negative (V_{Cd}^{2-}, a), single-negative (V_{Cd}^{1-}, b), and neutral (V_{Cd}^{0}, c) charge states. Tellurium atoms are shown in gold and cadmium vacancy center-of-mass in ocean blue, with each unique Te–V_{Cd} distance labeled. (Bottom) The corresponding electron energy level diagrams at the Γ point, with character symmetry labels. Superscripts b and a refer to bonding- and antibonding-type interactions, respectively.

neighboring Te atoms from the original bond distance of 2.83 Å to 2.61 Å from the vacancy center-of-mass.

The defect site distortions can be rationalized through consideration of the local bonding behavior in a molecular orbital model.[36,37] Removal of a Cd atom (and its two valence electrons) to create a vacancy results in a fully occupied A_1 electron level and a two-thirds occupied T_2 level at the Fermi level, arising from the tetrahedral coordination of Te sp^3-hybrid orbitals. In the double-negative case (V_{Cd}^{2-}), the T_2 level becomes fully occupied, and thus tetrahedral point symmetry is maintained (Figure 1a), with the Te atoms moving closer to the vacancy site to allow for greater hybridization between dangling bonds.

For the singly charged vacancy, the 5/6 partial occupancy of the T_2 level is unstable, undergoing a trigonal Jahn–Teller distortion that substantially elongates one of the Te neighbor distances (Figure 1b). In this C_{3v}-symmetry vacancy coordination, a positive hole is strongly localized on the Te atom furthest from the vacancy site, as depicted in Figure 2a, resulting in a paramagnetic defect species. This C_{3v} polaronic structure of V_{Cd}^{1-} was experimentally identified in the 1990s, using electron paramagnetic resonance (EPR),[14,16] but was only reproduced for the first time in a 2015 theoretical study by Shepidchenko et al.,[38] using the HSE06 functional. The primary reason why previous *ab initio* works[2,25,28,39–42] have failed to identify this polaronic ground-state structure for V_{Cd}^{1-} is the spurious electron self-interaction and consequent over-delocalization inherent in standard (semi)local DFT functionals.[20,43–45]

In the neutral case, we find that the Cd vacancy undergoes strong local relaxation to a C_{2v} structural motif, whereby two Te atoms move significantly closer both to the vacancy site and to each other (2.75 Å separation from an initial 4.63 Å) (Figure 1c). This yields a Te dimer arrangement with occupied sp^3 σ-bonding electronic levels deep in the valence band and unoccupied antibonding states in the conduction band (Figure 2b). Notably, this Te dimerization resembles that observed at low-energy surfaces and grain boundaries in CdTe and has been suggested as a source of fast recombination at these locations.[10,46,47] Similar metal–metal dimer reconstructions have been noted for neutral *anion* vacancies in the II–VI semiconductors ZnSe and ZnS,[48] occurring here for the *cation* vacancy in CdTe due to the metalloid character of the Te anion.

This atomic reconstruction reduces the vacancy formation energy by 0.52 eV, relative to the tetrahedral solution that has been widely reported[28,39–42,49–51] (Figures 3 and 4). As with

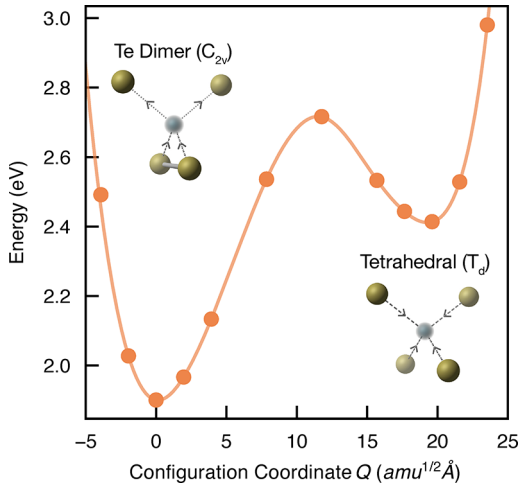

Figure 3. Potential energy surface for V_{Cd}^{0} along the configurational path from the "Te dimer" (Q = 0 $amu^{1/2}$ Å) to tetrahedral ($Q \simeq 20$ $amu^{1/2}$ Å) arrangement. Filled circles represent the calculated formation energies at a given configuration coordinate, and the solid line is a spline fit. Q is given in terms of mass-weighted displacement, and Te-rich conditions (μ_{Te} = 0) are assumed.

the C_{3v} Jahn–Teller distortion for V_{Cd}^{1-}, this Te dimer equilibrium structure of the neutral vacancy has only recently

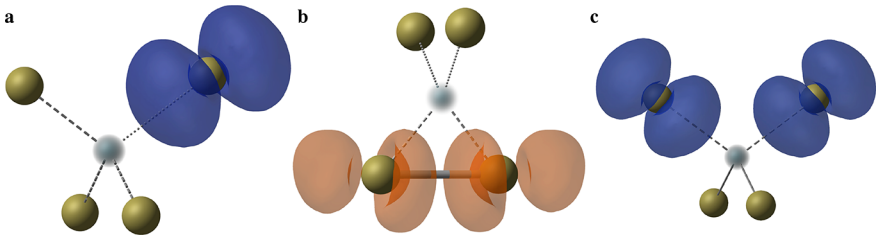

Figure 2. Spin-polarized charge-density isosurfaces of the localized hole polaron for the singly charged defect (V_{Cd}^{1-}, a), the unoccupied antibonding Te dimer state in the neutral vacancy (V_{Cd}^{0}, b), and the metastable high-spin bipolaron state for the neutral vacancy ($V_{Cd,Bipolaron}^{0}$, c). Tellurium atoms are shown in gold and cadmium vacancy center-of-mass in ocean blue. Isovalues are set to 0.006 e/Å^3 for the polarons (a, c) and 0.002 e/Å^3 for the dimer state (b).

https://doi.org/10.1021/acsenergylett.1c00380
ACS Energy Lett. 2021, 6, 1392–1398

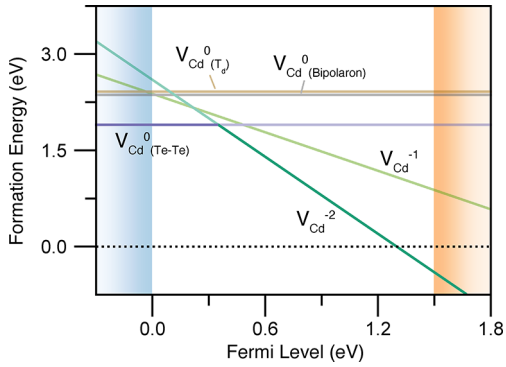

Figure 4. Defect formation energy diagram for the cadmium vacancy in CdTe, under Te-rich conditions ($\mu_{Te} = 0$), with the thermodynamically favored state for a given Fermi level (E_F) shown in saturated color. All locally stable configurations for the neutral vacancy are included.

been identified.[18] The tetrahedral and bipolaron (Figure 2c) configurations are in fact local minima on the defect potential energy surface (PES), as shown in Figures 3, 4, and S7.

The electronic behavior of the Cd vacancy is dramatically affected by Te dimerization, as the singly charged state V_{Cd}^{1-} is consequently predicted to be thermodynamically unfavorable across all Fermi energies (Figure 4). Accordingly, the vacancy is predicted to act as a so-called negative-U center,[52,53] with a single double-acceptor level at 0.35 eV above the valence band maximum (VBM). This is in excellent agreement with experimental reports of a single *thermal* ionization level in the bandgap at 0.3−0.4 eV above the VBM (Table S1).[29,31,32,54−58] Moreover, negative-U behavior helps to explain apparent discrepancies between experimental reports of Cd vacancy trap levels, as different techniques can measure either the single-charge (2− → 1− and 1− → 0) or double-charge transitions (2− → 0).[59] The reasons previous theoretical works have not identified this behavior are two-fold: namely, incomplete mapping of the defect potential energy surface (overlooking Te−Te dimerization in V_{Cd}^{0}) and qualitative errors in lower levels of electronic structure theory (destabilizing localized solutions; viz. the V_{Cd}^{1-} small-polaron); see Supporting Information, Section S6, for further discussion.

Optical Response. The paramagnetic nature of the single negative charge vacancy V_{Cd}^{1-} (due to the presence of an odd number of electrons) lends itself to experimental identification through electron spin resonance (ESR/EPR) spectroscopy. In 1993, Emanuelsson et al.[14] used photo-ESR to identify the C_{3v} coordination of V_{Cd}^{1-}, with a localized hole on a Te neighbor as predicted here (Figure 2a). After thermal annealing at 750 °C, they obtained a *p*-type CdTe film with a carrier concentration $p = 1.2 \times 10^{17}$ cm^{-3}, in excellent agreement with our predicted maximum hole concentration of $p = 4.2 \times 10^{17}$ cm^{-3} at this temperature (based on calculated intrinsic defect formation energies). While V_{Cd}^{1-} is never the lowest energy configuration at equilibrium, we find that Cd vacancies do in fact adopt this charge state under high-temperature *p*-type growth conditions, as a consequence of energy minimization within the constraint of charge neutrality (to counteract the large hole concentration).

Emanuelsson et al.[14] interpreted a decrease in the V_{Cd}^{1-} ESR intensity upon irradiation with photons of energy $h\nu > 0.47$ eV as the optical excitation of an electron from the valence band to the (−/2−) V_{Cd} level, to produce $V_{Cd}^{2-} + h_{VBM}^{+}$. Using the defect structures obtained in our investigations, we calculate the peak energy of this transition as 0.58 eV, with vibronic coupling estimated to give a Gaussian line shape with a fwhm of 0.12 eV, yielding good agreement with experiment (Figure 5).

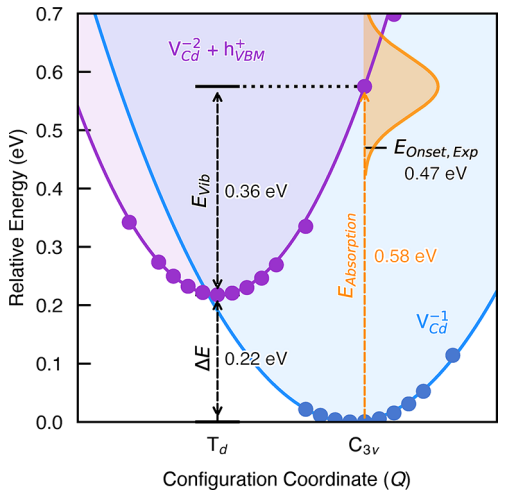

Figure 5. Configuration coordinate diagram for the $V_{Cd}^{1-} \rightarrow V_{Cd}^{2-}$ transition, showing the calculated optical excitation ($E_{Absorption}$) with vibrational broadening (orange curve), vibrational relaxation (E_{Vib}), thermodynamic transition (ΔE), and experimental absorption onset ($E_{Onset,Exp}$) energies. The solid lines are harmonic fits to the DFT energies, represented by filled circles. *X*-axis labels correspond to the defect point-group symmetry.

Trap-Mediated Recombination. To determine the non-radiative recombination activity, electron and hole capture coefficients were calculated for each charge state of the defect. This approach, building on the developments of Alkauskas et al.,[60] uses the CarrierCapture.jl package,[61] and full details of the calculation procedure are provided in the Supporting Information, Section S8. The PES of the defect is mapped along the structural path (configuration coordinate) Q between the equilibrium geometries for a given charge transition, from which nuclear wave function overlaps can be determined via the 1D Schrödinger equation.[60,62] Electron−phonon coupling is then calculated under static coupling perturbation theory which, in combination with phonon overlaps and scaling factors for charge interaction effects, yields the carrier capture coefficients $C_{p/n}^{q}$.

The energy surfaces for all in-gap V_{Cd} carrier traps are shown in Figure 6 and the resulting capture coefficients tabulated in the Supporting Information, Section S8. As expected for an acceptor defect with a trap level near the VBM (Figure 4), hole capture is fast while electron capture is slow for the (2−/−) transition, with small and large capture barriers, respectively. For the $V_{Cd}^{1-} \rightleftarrows V_{Cd}^{0}$ transitions, however, the behavior is drastically different to that predicted by a simple quantum defect model.[63] First, hole capture is more rapid than expected, due to the ability of V_{Cd}^{1-} to transition to the metastable $V_{Cd,Bipolaron}^{0}$ configuration, before relaxing to the $V_{Cd,Te\ Dimer}^{0}$ ground state. Second, despite the $(-/0)_{Te\ Dimer}$ trap level lying over 1 eV below the CBM (Figure 4), typically implying slow electron capture, we in fact find a giant electron capture coefficient. This unusual behavior is a direct result of the anharmonicity of the PESs at this trap center, accompanied by large electron−phonon coupling, through Te dimer formation.

https://doi.org/10.1021/acsenergylett.1c00380
ACS Energy Lett. 2021, 6, 1392−1398

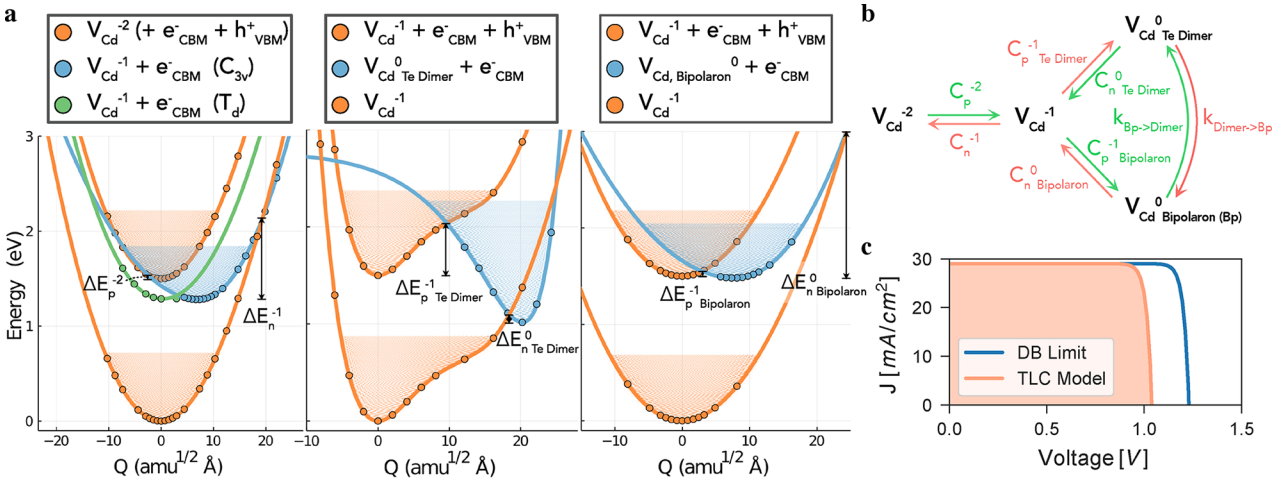

Figure 6. (a) Potential energy surfaces of the (2−/−) (left), $(-/0)_{\text{Te Dimer}}$ (center), and $(-/0)_{\text{Bipolaron}}$ (right) charge transitions for V_{Cd} in CdTe, with $\Delta E^{q}_{p/n}$ denoting the classical energy barrier to hole/electron capture by a vacancy in charge state q. Filled circles represent calculated energies, and the solid lines are best fits to the data. The vibrational wave functions are also shown. Q is the configurational coordinate path between equilibrium configurations, given in units of mass-weighted displacement. (b) Schematic of the non-radiative recombination mechanism at the cadmium vacancy, with the dominant (rapid) processes colored green. (c) $J-V$ curve for an ideal CdTe solar cell, based on the bulk electronic properties and excluding interfacial effects. "TLC" (trap-limited conversion efficiency) refers to a device limited by non-radiative recombination at V_{Cd} (details in text), and "DB" is the detailed balance limit.

These findings provide additional evidence to support Te dimerization at surfaces and grain boundaries in CdTe as a cause of high recombination velocities at these locations.[10,46,47] Consequently, the (−/0) V_{Cd} charge transition is predicted to facilitate rapid electron−hole recombination, proceeding via the $\{V^{1-}_{Cd} + e^{-}_{CBM} + h^{+}_{VBM}\} \rightarrow \{V^{0}_{Cd,Bipolaron} + e^{-}_{CBM}\} \rightarrow \{V^{0}_{Cd,Te\ Dimer} + e^{-}_{CBM}\} \rightarrow \{V^{1-}_{Cd}\}$ cycle shown in Figure 6b. Notably, the large capture coefficients for the rapid (green) processes are comparable to the most deleterious extrinsic defects in silicon[64,65] and the kesterite photovoltaic family.[62,66] This classifies V_{Cd} as a "killer center"[67] and demonstrates the potential impediment of this native defect species to the photovoltaic efficiency of untreated CdTe.

To quantify the effect of this recombination channel on CdTe solar cell performance, we calculate the trap-limited conversion efficiency (TLC),[66] which incorporates the effects of defect-mediated non-radiative recombination via the Shockley−Read−Hall model.[68] This allows us to set an upper limit on the achievable photovoltaic efficiency in the presence of defects. As depicted in the current−voltage curve in Figure 6c, we find that cadmium vacancies can significantly reduce the open-circuit voltage ($V_{OC,TLC}$ = 1.04 V), minority carrier lifetime (τ_e = 29 ns), and thus the maximum achievable photovoltaic efficiency from the ideal 32.1% to 26.7% (for intrinsic p-type CdTe processed under typical anneal temperatures of 600 °C in a Te-rich atmosphere, see Supporting Information, Section S8). Due to the large hole concentrations in the p-type compound, $V^{0}_{Cd,Te\ Dimer}$ will be the dominant state under steady-state illumination, with electron capture by this defect species representing the rate-limiting step:

$$R_{Total} \simeq R^{0}_{n,Te\ Dimer} = nC^{0}_{n}[V^{0}_{Cd,Te\ Dimer}]$$

Our prediction is a testament to the importance of Cl treatment, strategic impurity doping, and Cd-rich growth environments in the fabrication of high-efficiency CdTe devices,[9,11,32,34,69−79] which contribute to the passivation and reduction of cadmium vacancy populations. Notably, the recent achievement of open-circuit voltages surpassing the 1 V threshold for CdTe solar cells by Burst et al.[11] required a switch to an unorthodox strategy of Cd-rich growth conditions and group V anion doping, reducing the formation of V_{Cd} (and Te_{Cd}).

In conclusion, we reconcile several longstanding discrepancies between theoretical predictions and experimental measurements for CdTe, predicting both a single double-acceptor level and the C_{3v} V^{1-}_{Cd} hole−polaron state for the cadmium vacancy in CdTe. An equilibrium population of cadmium vacancies can facilitate rapid recombination of electrons and holes, reducing the maximum achievable power-conversion efficiency under idealized conditions by over 5%, for untreated CdTe. These recombination kinetics primarily arise from both metastable vacancy structures and the Te dimer configuration of V^{0}_{Cd} which, in addition to producing negative-U behavior, leads to anharmonic carrier capture PESs. Importantly, these results demonstrate the necessity to include the effects of both metastability and anharmonicity for the accurate calculation of charge-carrier recombination rates in photovoltaic materials.

■ ASSOCIATED CONTENT

Supporting Information

The Supporting Information is available free of charge at https://pubs.acs.org/doi/10.1021/acsenergylett.1c00380.

Computational methods; supporting notes S1 and S2; Figures S1−S3 and Tables S1−S4, showing bandgap-corrected hybrid DFT functional; bulk electronic structure; vacancy bonding, structural, and electronic analysis, including; discrepancies in theoretical studies; carrier capture model, results, and analysis, experimental identification of tellurium dimerization; defect electronic densities of states; and chemical potentials (PDF)

■ AUTHOR INFORMATION

Corresponding Authors

Aron Walsh − *Thomas Young Centre and Department of Materials, Imperial College London, London SW7 2AZ,*

https://doi.org/10.1021/acsenergylett.1c00380
ACS Energy Lett. 2021, 6, 1392−1398

U.K.; Department of Materials Science and Engineering, Yonsei University, Seoul 03722, Republic of Korea; orcid.org/0000-0001-5460-7033; Email: a.walsh@imperial.ac.uk

David O. Scanlon − *Thomas Young Centre and Department of Chemistry, University College London, London WC1H 0AJ, U.K.; Diamond Light Source Ltd., Didcot, Oxfordshire OX11 0DE, U.K.;* orcid.org/0000-0001-9174-8601; Email: d.scanlon@ucl.ac.uk

Author

Seán R. Kavanagh − *Thomas Young Centre and Department of Chemistry, University College London, London WC1H 0AJ, U.K.; Thomas Young Centre and Department of Materials, Imperial College London, London SW7 2AZ, U.K.;* orcid.org/0000-0003-4577-9647

Complete contact information is available at: https://pubs.acs.org/10.1021/acsenergylett.1c00380

Notes

The authors declare no competing financial interest.

Data produced during this work is freely available at https://zenodo.org/record/4541602.

■ ACKNOWLEDGMENTS

We thank Dr. Anna Lindström for valuable discussions regarding polaronic structures for cadmium vacancies, and Dr. Sungyhun Kim for assistance with CarrierCapture.jl calculations. S.R.K. acknowledges the EPSRC Centre for Doctoral Training in the Advanced Characterisation of Materials (CDT-ACM)(EP/S023259/1) for funding a Ph.D. studentship. We acknowledge the use of the UCL Grace High Performance Computing Facility (Grace@UCL), the Imperial College Research Computing Service, and associated support services, in the completion of this work. Via membership of the UK's HEC Materials Chemistry Consortium, which is funded by the EPSRC (EP/L000202, EP/R029431, EP/T022213), this work used the ARCHER UK National Supercomputing Service (www.archer.ac.uk and the UK Materials and Molecular Modelling (MMM) Hub (Thomas EP/P020194 and Young EP/T022213).

■ REFERENCES

(1) Zidane, T. E. K.; Adzman, M. R. B.; Tajuddin, M. F. N.; Mat Zali, S.; Durusu, A. Optimal Configuration of Photovoltaic Power Plant Using Grey Wolf Optimizer: A Comparative Analysis Considering CdTe and c-Si PV Modules. *Sol. Energy* **2019**, *188*, 247−257.

(2) Yang, J.-H.; Yin, W.-J.; Park, J.-S.; Ma, J.; Wei, S.-H. Review on First-Principles Study of Defect Properties of CdTe as a Solar Cell Absorber. *Semicond. Sci. Technol.* **2016**, *31*, 083002.

(3) First Solar Press Release: First Solar Achieves Yet Another Cell Conversion Efficiency World Record, Feb 23, 2016, investor.firstsolar.com/news/press-release-details/2016/First-Solar-Achieves-Yet-Another-Cell-Conversion-Efficiency-World-Record (accessed March 11, 2021).

(4) NREL Photovoltaic Research: Best Research-Cell Efficiency Chart, nrel.gov/pv/cell-efficiency.html (accessed March 11, 2021).

(5) Durose, K.; Edwards, P. R.; Halliday, D. P. Materials Aspects of CdTe/CdS Solar Cells. *J. Cryst. Growth* **1999**, *197*, 733−742.

(6) Geisthardt, R. M.; Topič, M.; Sites, J. R. Status and Potential of CdTe Solar-Cell Efficiency. *IEEE Journal of Photovoltaics* **2015**, *5*, 1217−1221.

(7) Shockley, W.; Queisser, H. J. Detailed Balance Limit of Efficiency of P-n Junction Solar Cells. *J. Appl. Phys.* **1961**, *32*, 510−519.

(8) Pan, J.; Metzger, W. K.; Lany, S. Spin-Orbit Coupling Effects on Predicting Defect Properties with Hybrid Functionals: A Case Study in CdTe. *Phys. Rev. B: Condens. Matter Mater. Phys.* **2018**, *98*, 054108.

(9) Ma, J.; Kuciauskas, D.; Albin, D.; Bhattacharya, R.; Reese, M.; Barnes, T.; Li, J. V.; Gessert, T.; Wei, S.-H. Dependence of the Minority-Carrier Lifetime on the Stoichiometry of CdTe Using Time-Resolved Photoluminescence and First-Principles Calculations. *Phys. Rev. Lett.* **2013**, *111*, 067402.

(10) Reese, M. O.; Perkins, C. L.; Burst, J. M.; Farrell, S.; Barnes, T. M.; Johnston, S. W.; Kuciauskas, D.; Gessert, T. A.; Metzger, W. K. Intrinsic Surface Passivation of CdTe. *J. Appl. Phys.* **2015**, *118*, 155305.

(11) Burst, J. M.; Duenow, J. N.; Albin, D. S.; Colegrove, E.; Reese, M. O.; Aguiar, J. A.; Jiang, C.-S.; Patel, M. K.; Al-Jassim, M. M.; Kuciauskas, D.; Swain, S.; Ablekim, T.; Lynn, K. G.; Metzger, W. K. CdTe Solar Cells with Open-Circuit Voltage Breaking the 1 V Barrier. *Nature Energy* **2016**, *1*, 16015.

(12) Castaldini, A.; Cavallini, A.; Fraboni, B.; Fernandez, P.; Piqueras, J. Deep Energy Levels in CdTe and CdZnTe. *J. Appl. Phys.* **1998**, *83*, 2121−2126.

(13) Mathew, X. Photo-Induced Current Transient Spectroscopic Study of the Traps in CdTe. *Sol. Energy Mater. Sol. Cells* **2003**, *76*, 225−242.

(14) Emanuelsson, P.; Omling, P.; Meyer, B. K.; Wienecke, M.; Schenk, M. Identification of the Cadmium Vacancy in CdTe by Electron Paramagnetic Resonance. *Phys. Rev. B: Condens. Matter Mater. Phys.* **1993**, *47*, 15578−15580.

(15) Kröger, F. The Defect Structure of CdTe. *Rev. Phys. Appl.* **1977**, *12*, 205−210.

(16) Meyer, B. K.; Hofmann, D. M. Anion and Cation Vacancies in CdTe. *Appl. Phys. A: Mater. Sci. Process.* **1995**, *61*, 213−215.

(17) Meyer, B. K.; Omling, P.; Weigel, E.; Müller-Vogt, G. *F* Center in CdTe. *Phys. Rev. B: Condens. Matter Mater. Phys.* **1992**, *46*, 15135−15138.

(18) Lindström, A.; Mirbt, S.; Sanyal, B.; Klintenberg, M. High Resistivity in Undoped CdTe: Carrier Compensation of Te Antisites and Cd Vacancies. *J. Phys. D: Appl. Phys.* **2016**, *49*, 035101.

(19) Whelan, R. C.; Shaw, D. Evidence of a Doubly Ionized Native Donor in CdTe. *Phys. Status Solidi B* **1968**, *29*, 145−152.

(20) Huang, Y.-T.; Kavanagh, S. R.; Scanlon, D. O.; Walsh, A.; Hoye, R. L. Z. Perovskite-Inspired Materials for Photovoltaics and beyond− from Design to Devices. *Nanotechnology* **2021**, *32*, 132004.

(21) Li, Z.; Kavanagh, S. R.; Napari, M.; Palgrave, R. G.; Abdi-Jalebi, M.; Andaji-Garmaroudi, Z.; Davies, D. W.; Laitinen, M.; Julin, J.; Isaacs, M. A.; Friend, R. H.; Scanlon, D. O.; Walsh, A.; Hoye, R. L. Z. Bandgap Lowering in Mixed Alloys of $Cs_2Ag(Sb_xBi_{1-x})Br_6$ Double Perovskite Thin Films. *J. Mater. Chem. A* **2020**, *8*, 21780−21788.

(22) Rau, U.; Blank, B.; Müller, T. C. M.; Kirchartz, T. Efficiency Potential of Photovoltaic Materials and Devices Unveiled by Detailed-Balance Analysis. *Phys. Rev. Appl.* **2017**, *7*, 044016.

(23) Green, M. A. Radiative Efficiency of State-of-the-Art Photovoltaic Cells. *Prog. Photovoltaics* **2012**, *20*, 472−476.

(24) Meyer, B. K.; Stadler, W. Native Defect Identification in II−VI Materials. *J. Cryst. Growth* **1996**, *161*, 119−127.

(25) Carvalho, A.; Tagantsev, A. K.; Öberg, S.; Briddon, P. R.; Setter, N. Cation-Site Intrinsic Defects in Zn-Doped CdTe. *Phys. Rev. B: Condens. Matter Mater. Phys.* **2010**, *81*, 075215.

(26) Menéndez-Proupin, E.; Amézaga, A.; Cruz Hernández, N. Electronic Structure of CdTe Using GGA+USIC. *Phys. B* **2014**, *452*, 119−123.

(27) Menéndez-Proupin, E.; Orellana, W. Theoretical Study of Intrinsic Defects in CdTe. *J. Phys.: Conf. Ser.* **2016**, *720*, 012031.

(28) Wei, S.-H.; Zhang, S. B.; Zunger, A. First-Principles Calculation of Band Offsets, Optical Bowings, and Defects in CdS, CdSe, CdTe, and Their Alloys. *J. Appl. Phys.* **2000**, *87*, 1304−1311.

(29) Takebe, T.; Hirata, T.; Saraie, J.; Matsunami, H. DLTS Studies of Deep Levels in Semiconducting N-CdTe Single Crystals. *J. Phys. Chem. Solids* **1982**, *43*, 5−12.
(30) Shepidchenko, A.; Mirbt, S.; Sanyal, B.; HÅkansson, A.; Klintenberg, M. Tailoring of Defect Levels by Deformations: Te-Antisite in CdTe. *J. Phys.: Condens. Matter* **2013**, *25*, 415801.
(31) Reislöhner, U.; Grillenberger, J.; Witthuhn, W. Band-Gap Level of the Cadmium Vacancy in CdTe. *J. Cryst. Growth* **1998**, *184−185*, 1160−1164.
(32) Szeles, C.; Shan, Y. Y.; Lynn, K. G.; Moodenbaugh, A. R.; Eissler, E. E. Trapping Properties of Cadmium Vacancies in $Cd_{1-x}Zn_xTe$. *Phys. Rev. B: Condens. Matter Mater. Phys.* **1997**, *55*, 6945−6949.
(33) Walsh, A.; Zunger, A. Instilling Defect Tolerance in New Compounds. *Nat. Mater.* **2017**, *16*, 964−967.
(34) Park, J. S.; Kim, S.; Xie, Z.; Walsh, A. Point Defect Engineering in Thin-Film Solar Cells. *Nature Reviews Materials* **2018**, *3*, 194−210.
(35) Scanlon, D. O.; Morgan, B. J.; Watson, G. W.; Walsh, A. Acceptor Levels in *P*-Type Cu_2O: Rationalizing Theory and Experiment. *Phys. Rev. Lett.* **2009**, *103*, 096405.
(36) Watkins, G. Lattice Defects in II-VI Compounds. In *Radiation Effects in Semiconductors*, papers from the International Conference on Radiation Effects in Semiconductors, Dubrovnik, Croatia, Sept 6−9, 1976; Urli, N. B., Corbett, J. W., Eds.; Institute of Physics: London, 1977; p 95.
(37) Watkins, G. Intrinsic Defects in II−VI Semiconductors. *J. Cryst. Growth* **1996**, *159*, 338−344.
(38) Shepidchenko, A.; Sanyal, B.; Klintenberg, M.; Mirbt, S. Small Hole Polaron in CdTe: Cd-Vacancy Revisited. *Sci. Rep.* **2015**, *5*, 14509.
(39) Du, M.-H.; Takenaka, H.; Singh, D. J. Carrier Compensation in Semi-Insulating CdTe: First-Principles Calculations. *Phys. Rev. B: Condens. Matter Mater. Phys.* **2008**, *77*, 094122.
(40) Chang, Y.-C.; James, R. B.; Davenport, J. W. Symmetrized-Basis LASTO Calculations of Defects in CdTe and ZnTe. *Phys. Rev. B: Condens. Matter Mater. Phys.* **2006**, *73*, 035211.
(41) Lordi, V. Point Defects in Cd(Zn)Te and TlBr: Theory. *J. Cryst. Growth* **2013**, *379*, 84−92.
(42) Biswas, K.; Du, M.-H. What Causes High Resistivity in CdTe. *New J. Phys.* **2012**, *14*, 063020.
(43) Alberi, K. The 2019 Materials by Design Roadmap. *J. Phys. D: Appl. Phys.* **2019**, *52*, 013001.
(44) Butler, K. T.; Davies, D. W.; Walsh, A. In *Computational Materials Discovery*; Oganov, A. R., Saleh, G., Kvashnin, A. G., Eds.; Royal Society of Chemistry: Cambridge, 2018; pp 176−197.
(45) Freysoldt, C.; Grabowski, B.; Hickel, T.; Neugebauer, J.; Kresse, G.; Janotti, A.; Van de Walle, C. G. First-Principles Calculations for Point Defects in Solids. *Rev. Mod. Phys.* **2014**, *86*, 253−305.
(46) Mönch, W. *Semiconductor Surfaces and Interfaces*, 3rd ed.; Springer Series in Surface Sciences; Springer-Verlag: Berlin, Heidelberg, 2001.
(47) Ahr, M.; Biehl, M. Flat (001) Surfaces of II−VI Semiconductors: A Lattice Gas Model. *Surf. Sci.* **2002**, *505*, 124−136.
(48) Lany, S.; Zunger, A. Metal-Dimer Atomic Reconstruction Leading to Deep Donor States of the Anion Vacancy in II-VI and Chalcopyrite Semiconductors. *Phys. Rev. Lett.* **2004**, *93*, 156404.
(49) Lany, S.; Ostheimer, V.; Wolf, H.; Wichert, T. Vacancies in CdTe: Experiment and Theory. *Phys. B* **2001**, *308−310*, 958−962.
(50) Chanier, T.; Opahle, I.; Sargolzaei, M.; Hayn, R.; Lannoo, M. Magnetic State around Cation Vacancies in II-VI Semiconductors. *Phys. Rev. Lett.* **2008**, *100*, 026405.
(51) Xu, R.; Xu, H.-T.; Tang, M.-Y.; Wang, L.-J. Hybrid Density Functional Studies of Cadmium Vacancy in CdTe. *Chin. Phys. B* **2014**, *23*, 077103.
(52) Watkins, G. D. In *Advances in Solid State Physics*; Grosse, P., Ed.; Springer: Berlin, Heidelberg, 1984; Vol. *24*, pp 163−189.
(53) Coutinho, J.; Markevich, V. P.; Peaker, A. R. Characterisation of Negative- *U* Defects in Semiconductors. *J. Phys.: Condens. Matter* **2020**, *32*, 323001.
(54) Vul, B.; Vavilov, V.; Ivanov, V.; Stopachinskii, V.; Chapnin, V. Investigation of Doubly Charged Acceptors in Cadmium Telluride. *Soviet Physics Semiconductors - USSR* **1973**, *6*, 1255−1258.
(55) Gippius, A. A.; Panossian, J. R.; Chapnin, V. A. Deep-Centre Ionization Energies in CdTe Determined from Electrical and Optical Measurements. *Physica Status Solidi (a)* **1974**, *21*, 753−758.
(56) Scholz, K.; Stiens, H.; Müller-Vogt, G. Investigations on the Effect of Contacts on P-Type CdTe DLTS-Measurements. *J. Cryst. Growth* **1999**, *197*, 586−592.
(57) Becerril, M.; Zelaya-Angel, O.; Vargas-García, J. R.; Ramírez-Bon, R.; González-Hernández, J. Effects of Cd Vacancies on the Electrical Properties of Polycrystalline CdTe Sputtered Films. *J. Phys. Chem. Solids* **2001**, *62*, 1081−1085.
(58) Kremer, R.; Leigh, W. Deep Levels in CdTe. *J. Cryst. Growth* **1988**, *86*, 490−496.
(59) Wickramaratne, D.; Dreyer, C. E.; Monserrat, B.; Shen, J.-X.; Lyons, J. L.; Alkauskas, A.; Van de Walle, C. G. Defect Identification Based on First-Principles Calculations for Deep Level Transient Spectroscopy. *Appl. Phys. Lett.* **2018**, *113*, 192106.
(60) Alkauskas, A.; Yan, Q.; Van de Walle, C. G. First-Principles Theory of Nonradiative Carrier Capture via Multiphonon Emission. *Phys. Rev. B: Condens. Matter Mater. Phys.* **2014**, *90*, 075202.
(61) Kim, S.; Hood, S. N.; van Gerwen, P.; Whalley, L. D.; Walsh, A. CarrierCapture.Jl: Anharmonic Carrier Capture. *Zenodo* **2020**, 3707592.
(62) Kim, S.; Hood, S. N.; Walsh, A. Anharmonic Lattice Relaxation during Nonradiative Carrier Capture. *Phys. Rev. B: Condens. Matter Mater. Phys.* **2019**, *100*, 041202.
(63) Das, B.; Aguilera, I.; Rau, U.; Kirchartz, T. What Is a Deep Defect? Combining Shockley-Read-Hall Statistics with Multiphonon Recombination Theory. *Physical Review Materials* **2020**, *4*, 024602.
(64) Macdonald, D.; Geerligs, L. J. Recombination Activity of Interstitial Iron and Other Transition Metal Point Defects in P- and n-Type Crystalline Silicon. *Appl. Phys. Lett.* **2004**, *85*, 4061−4063.
(65) Peaker, A. R.; Markevich, V. P.; Hamilton, B.; Parada, G.; Dudas, A.; Pap, A.; Don, E.; Lim, B.; Schmidt, J.; Yu, L.; Yoon, Y.; Rozgonyi, G. Recombination via Point Defects and Their Complexes in Solar Silicon. *Phys. Status Solidi A* **2012**, *209*, 1884−1893.
(66) Kim, S.; Márquez, J. A.; Unold, T.; Walsh, A. Upper Limit to the Photovoltaic Efficiency of Imperfect Crystals from First Principles. *Energy Environ. Sci.* **2020**, *13*, 1481−1491.
(67) Stoneham, A. M. *Theory of Defects in Solids: Electronic Structure of Defects in Insulators and Semiconductors*; Oxford University Press: London, 2001.
(68) Shockley, W.; Read, W. T. Statistics of the Recombinations of Holes and Electrons. *Phys. Rev.* **1952**, *87*, 835−842.
(69) Metzger, W. K.; et al. Exceeding 20% Efficiency with in Situ Group V Doping in Polycrystalline CdTe Solar Cells. *Nature Energy* **2019**, *4*, 837−845.
(70) Yang, J.-H.; Yin, W.-J.; Park, J.-S.; Burst, J.; Metzger, W. K.; Gessert, T.; Barnes, T.; Wei, S.-H. Enhanced P-Type Dopability of P and As in CdTe Using Non-Equilibrium Thermal Processing. *J. Appl. Phys.* **2015**, *118*, 025102.
(71) Amarasinghe, M.; Colegrove, E.; Moseley, J.; Moutinho, H.; Albin, D.; Duenow, J.; Jensen, S.; Kephart, J.; Sampath, W.; Sivananthan, S.; Al-Jassim, M.; Metzger, W. K. Obtaining Large Columnar CdTe Grains and Long Lifetime on Nanocrystalline CdSe, MgZnO, or CdS Layers. *Adv. Energy Mater.* **2018**, *8*, 1702666.
(72) Moseley, J.; Rale, P.; Collin, S.; Colegrove, E.; Guthrey, H.; Kuciauskas, D.; Moutinho, H.; Al-Jassim, M.; Metzger, W. K. Luminescence Methodology to Determine Grain-Boundary, Grain-Interior, and Surface Recombination in Thin-Film Solar Cells. *J. Appl. Phys.* **2018**, *124*, 113104.
(73) Major, J. D.; Treharne, R. E.; Phillips, L. J.; Durose, K. A Low-Cost Non-Toxic Post-Growth Activation Step for CdTe Solar Cells. *Nature* **2014**, *511*, 334−337.

https://doi.org/10.1021/acsenergylett.1c00380
ACS Energy Lett. 2021, 6, 1392−1398

(74) Metzger, W. K.; Albin, D.; Levi, D.; Sheldon, P.; Li, X.; Keyes, B. M.; Ahrenkiel, R. K. Time-Resolved Photoluminescence Studies of CdTe Solar Cells. *J. Appl. Phys.* **2003**, *94*, 3549−3555.
(75) Moutinho, H. R.; Al-Jassim, M. M.; Levi, D. H.; Dippo, P. C.; Kazmerski, L. L. Effects of CdCl2 Treatment on the Recrystallization and Electro-Optical Properties of CdTe Thin Films. *J. Vac. Sci. Technol., A* **1998**, *16*, 1251−1257.
(76) Kranz, L.; et al. Doping of Polycrystalline CdTe for High-Efficiency Solar Cells on Flexible Metal Foil. *Nat. Commun.* **2013**, *4*, 2306.
(77) Gessert, T. A.; Wei, S. H.; Ma, J.; Albin, D. S.; Dhere, R. G.; Duenow, J. N.; Kuciauskas, D.; Kanevce, A.; Barnes, T. M.; Burst, J. M.; Rance, W. L.; Reese, M. O.; Moutinho, H. R. Research Strategies toward Improving Thin-Film CdTe Photovoltaic Devices beyond 20% Conversion Efficiency. *Sol. Energy Mater. Sol. Cells* **2013**, *119*, 149−155.
(78) Komin, V.; Tetali, B.; Viswanathan, V.; Yu, S.; Morel, D. L.; Ferekides, C. S. The Effect of the CdCl2 Treatment on CdTe/CdS Thin Film Solar Cells Studied Using Deep Level Transient Spectroscopy. *Thin Solid Films* **2003**, *431−432*, 143−147.
(79) Kanevce, A.; Reese, M. O.; Barnes, T. M.; Jensen, S. A.; Metzger, W. K. The Roles of Carrier Concentration and Interface, Bulk, and Grain-Boundary Recombination for 25% Efficient CdTe Solar Cells. *J. Appl. Phys.* **2017**, *121*, 214506.

https://doi.org/10.1021/acsenergylett.1c00380
ACS Energy Lett. 2021, 6, 1392−1398